Ultramicroscopy 000 (2017) 1–6

Contents lists available at ScienceDirect

Ultramicroscopy

journal homepage: www.elsevier.com/locate/ultramic

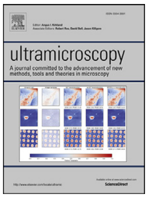

Electron-beam-induced-current and active secondary-electron voltage-contrast with aberration-corrected electron probes

Myung-Geun Han[a,*], Joseph A. Garlow[a,b], Matthew S.J. Marshall[c], Amanda L. Tiano[c], Stanislaus S. Wong[a,c], Sang-Wook Cheong[d], Frederick J. Walker[e,f], Charles H. Ahn[e,f], Yimei Zhu[a]

[a] Condensed Matter Physics & Materials Science, Brookhaven National Laboratory, Upton, NY 11973, USA
[b] Materials Science and Engineering Department, Stony Brook University, Stony Brook, NY 11794, USA
[c] Department of Chemistry, Stony Brook University, Stony Brook, NY 11974, USA
[d] Department of Physics and Astronomy, Rutgers Center for Emergent Materials, Rutgers University, Piscataway, NJ 08854, USA
[e] Department of Applied Physics and Center for Research on Interface Structures and Phenomena, Yale University, New Haven, CT 06520, USA
[f] Department of Mechanical Engineering and Materials Science, Yale University, New Haven, CT 06520, USA

ARTICLE INFO

Article history:
Received 25 September 2016
Revised 3 January 2017
Accepted 22 January 2017
Available online xxx

Keywords:
Electron holography
Electric biasing
Ferroelectric
Electrostatic potential

ABSTRACT

The ability to map out electrostatic potentials in materials is critical for the development and the design of nanoscale electronic and spintronic devices in modern industry. Electron holography has been an important tool for revealing electric and magnetic field distributions in microelectronics and magnetic-based memory devices, however, its utility is hindered by several practical constraints, such as charging artifacts and limitations in sensitivity and in field of view. In this article, we report electron-beam-induced-current (EBIC) and secondary-electron voltage-contrast (SE-VC) with an aberration-corrected electron probe in a transmission electron microscope (TEM), as complementary techniques to electron holography, to measure electric fields and surface potentials, respectively. These two techniques were applied to ferroelectric thin films, multiferroic nanowires, and single crystals. Electrostatic potential maps obtained by off-axis electron holography were compared with EBIC and SE-VC to show that these techniques can be used as a complementary approach to validate quantitative results obtained from electron holography analysis.

Nanoscale control of electric fields in modern electronic devices is a prerequisite to improving their functionalities in conjunction with the scaling demand for high-density semiconductor devices. One of the key factors is interfaces/junctions, where built-in electric fields are generally predicted. At thermal equilibrium, the necessity of Fermi level equilibration across interfaces/junctions requires charge exchange, leaving net space charges on either one or both sides of the interface. These space charges yield built-in electric fields that prevent further charge exchange across the interface/junction. Experimental measurements of these built-in electric fields are of great importance to predict and control charge transport properties in advanced devices that involve photovoltaic effects, rectifications, or capacitance modulations, etc.

In electron microscopy, off-axis electron holography has been an important tool for mapping 2D electric fields in sub-micrometer semiconductor field-effect transistors, semiconductor nanowires, and nanocrystals, etc. [1–5]. However, practical limitations in addition to the stringent requirements of TEM sample preparation limit the efficacy of off-axis electron holography. When the sample is charging, the reference wave coming from vacuum in proximity to the area of interest is disturbed, thereby preventing reliable quantitative analysis [6]. In addition, requirements on the lens conditions limit the available field of view and spatial resolution [1].

Meanwhile, both EBIC and SE-VC have been widely utilized to study correlations between electronic properties and structural defects as well as failure analysis in semiconductor devices [7–10]. These two techniques have been mainly performed in a scanning electron microscope (SEM), however, there are also numerous studies that have been performed in a scanning transmission electron microscope (STEM) [11–14]. The difficulty here is that electrical connection to a TEM sample is a challenging task. When 200 keV electrons are passing through a TEM sample, they generate electron hole pairs (ehps) and secondary electrons via inelastic scattering processes. Previously, we have shown that each 200 keV electron can generate ~100 electron hole pairs in crystalline Si [15]. The ehps are excess charge carriers, which eventually recombine to annihilate each other with a characteristic time scale, called

---

[*] Corresponding author.
E-mail address: mghan@bnl.gov (M.-G. Han).

http://dx.doi.org/10.1016/j.ultramic.2017.03.028
0304-3991/© 2017 Published by Elsevier B.V.

excess carrier lifetime. During this lifetime, these carriers may diffuse in random directions before recombination. When semiconductors are doped, either *n*-type (electrons being a majority charge carrier) or *p*-type (holes being a majority charge carrier), the ehps lifetime is determined by the minority carrier lifetime because there are so many majority carriers that are available for recombination.

When there is an electric field, either externally applied or built-in, as in the depletion region at either a *p-n* junction or a Schottky junction, electrons and holes move in opposite directions and, thus, generate a current (EBIC) in the direction of the field. This induced current for each scanning electron beam synchronized with STEM coils is measured and used as the imaging signal to acquire an EBIC image. As a result, the EBIC intensity is proportional to the magnitude of local electric fields for a given excitation. Commercial SEM-based systems afford a minimum current down to 0.8 fA using a lock-in technique [16]. The minimum measurable current in this study is in the range of a few tens of pico-Amperes without lock-in filtering.

SE-VC has been extensively utilized, especially to localize failure sites in integrated semiconductor circuits. Generally, different intensities in SEM images help to identify electrical shorts and/or disconnects in circuits. For this “passive” VC case, it is not necessary to apply an external bias. However, the intensity differences can be more pronounced if an external bias is applied to the circuit under test. This is because the secondary electron yield is not only sensitive to the incoming electron energy, but also to local electrostatic potentials for a given material. When a positive (negative) external bias is applied to the material, the secondary electron yield is suppressed (enhanced) by simple electrostatic interactions. This “active” VC method can detect the failures occurring in a device under operating conditions.

A key advantage of EBIC and SE-VC with thin TEM samples is that the interaction volume is small due to reduced electron beam broadening. Therefore, the spatial resolution is not degraded by SEs generated by backscattered electrons (called “SE2”) but is mainly determined by SEs generated by the primary imaging electrons (“SE1”). This means that the spatial resolution of SEM on TEM samples is comparable to the probe size. With aberration-corrected electron probes, indeed atomic resolution has previously been demonstrated [17,18]. Another advantage of TEM samples is that the sample thickness is comparable to the escape depth of SE emission from both the top and bottom surfaces of the TEM sample. Ehp recombination at the top and bottom surface regions is also quite fast as compared with bulk and the surfaces likely serve as recombination centers. It should be noted that SE-VC imaging is sensitive to the sample surface, thus, the potential probed by SE-VC may be different from potentials for the bulk.

In this article, we present electron-beam-induced-current (EBIC) measurement and secondary-electron voltage-contrast (SE-VC) obtained in STEM mode combined with *in situ* electrical biasing in a TEM. These techniques were applied to ferroelectric thin films, nanowires, and single crystals. A comparison with off-axis electron holography data demonstrates that although EBIC and SE-VC data are currently qualitative, they can be used as complementary measurements to support quantitative data obtained by off-axis electron holography.

We have used double aberration-corrected JEOL ARM 200 CF with cold field-emission gun. The electrical connection to TEM samples for EBIC and SE-VC was made using a commercial TEM holder (Nanofactory Instruments). The probe current density was about 0.22 nA/nm^2 for both EBIC and SE-VC experiments. EBIC signals were acquired simultaneously with STEM-HAADF images obtained with acceptance angles ranging from 68 to 280 mrad. Fig. 1 shows a schematic of EBIC and SE-VC measurements in STEM mode. The horizontal stripes in the EBIC image shown in Fig. 1 are artifacts that arise during EBIC signal acquisition and can be removed by adjusting signal amplification in the data collecting electronics (Gatan Digiscan II). We have used a JEOL backscattered electron detector for SE-VC imaging. The detectors are composed of two segments and collect not only SE, but also backscattered electrons, though, most of electrons detected are primarily SEs (85%). As EBIC and SE-VC detectors are not interfering with HAADF and BF STEM detectors, all four images can be simultaneously acquired.

We have prepared a FIB-milled TEM sample of a $PbZr_{0.2}Ti_{0.8}O_3$ (PZT) thin film grown onto conducting Nb-doped (001) $SrTiO_3$ (Nb-STO) substrates, as shown in Fig. 2 (a). The sample is divided into two parts using a FIB cut (v-shape cut in the center part). One section on the left hand side in Fig. 2(a) is in the ‘open-circuit’ configuration as the top electrode is floated while the bottom electrode (conducting Nb-STO) is connected to the voltage source. The other section on the right is in the ‘closed-circuit’ configuration as the top and bottom electrodes are electrically connected each other by a molybdenum TEM grid (Omniprobe, Inc.). An electric contact was made to the open-circuited section with a tungsten probe using a commercial Nanofactory holder. Previously, we have shown that the PZT/Nb-STO interface behaves like a *p-n* junction, preventing polarization from switching at the interface when the polarization direction is parallel to the interfacial built-in electric field [19]. In Fig. 2(c) and (e), EBIC images taken from the two sections of the PZT/Nb-STO interface are shown together with HAADF images that were simultaneously acquired. A positive 2 V potential was applied to the Nb-STO substrate while the tungsten probe was grounded during the image acquisition. The EBIC signal is clearly seen at the interface of PZT/Nb-STO in the open-circuit configuration (Fig. 2(c)), while the EBIC signal was not observed for the ‘closed-circuit’ configuration (Fig. 2(e)). In Fig. 2(f), the line profiles of EBIC signals are plotted as a function of applied bias to the Nb-STO substrate are shown. As a small positive voltage is applied to the *n*-type Nb-STO, the PZT/Nb-STO is reversely biased. As a result, the depletion region across the interface is expanded to give larger EBIC signals. In contrast, for the ‘closed-circuit’ section, although there is a small built-in electric field across the PZT/Nb-STO interface to separate ehps, EBIC was not observed, as shown in Fig. 2(e). These results demonstrate that EBIC is not an artifact of STEM imaging and requires proper electrical connection to the TEM samples. As discussed previously, the EBIC signal can broaden due to ehp diffusion before collection as a current. By comparing Holography data with EBIC data shown in Fig. 2(f) and (g), respectively, we have found that the ehp diffusion length for FIB-milled STO can be roughly estimated as ~300 nm (for positive 2 V, about 300 nm depletion region by EBIC and for positive 3 V, 50 nm by EH). Finally, it is interesting to note that the depletion region in PZT is fixed around 30 nm and narrower than that on the STO side. This may be associated with spontaneous polarization, charged defects (oxygen/cation vacancies and cation impurities) and their electric dipoles in the PZT film, which may limit the expansion of the PZT depletion region.

Active SE-VC has been performed on the same sample, as shown in Fig. 3(b-d). The brightness of image depends upon the external bias applied to the Nb-STO substrate with respect to the grounded top electrode. For example, when a positive 4 V potential is applied, the brightness of Nb-STO substrate is decreased with respect to the top electrode. On the other hand, when a negative 3 V potential is applied, the signal brightness of Nb-STO is enhanced. The brightness is also sensitive to the surface conditions of the TEM sample. When a sample is slightly contaminated by mainly hydrocarbons during extensive imaging, we have observed the SE image brightness is reduced. In Fig. 3(d), there is a rectangular area with suppressed contrast in the Nb-STO substrate due to surface contamination by extensive electron beam scanning. When there is no significant surface contamination,

Please cite this article as: M.-G. Han et al., Electron-beam-induced-current and active secondary-electron voltage-contrast with aberration-corrected electron probes, Ultramicroscopy (2017), http://dx.doi.org/10.1016/j.ultramic.2017.03.028